NASA TECHNICAL NOTE

NASA TN D-5191

EXPERIMENTS ON ROTATING EXTERNALLY PRESSURIZED, AIR JOURNAL BEARINGS

I — Load Capacity and Stiffness

by Robert E. Cunningham, David P. Fleming, and William J. Anderson

Lewis Research Center
Cleveland, Ohio

NATIONAL AERONAUTICS AND SPACE ADMINISTRATION • WASHINGTON, D. C. • JUNE 1969

NASA TN D-5191

EXPERIMENTS ON ROTATING EXTERNALLY PRESSURIZED, AIR JOURNAL BEARINGS

I - Load Capacity and Stiffness

By Robert E. Cunningham, David P. Fleming, and William J. Anderson

Lewis Research Center
Cleveland, Ohio

NATIONAL AERONAUTICS AND SPACE ADMINISTRATION

For sale by the Clearinghouse for Federal Scientific and Technical Information
Springfield, Virginia 22151 – CFSTI price $3.00

ABSTRACT

Experimental load and stiffness data for a pair of $2\frac{1}{2}$-in. (6.3-cm) diameter, $3\frac{3}{4}$-in. (9.5-cm) long externally pressurized air journal bearings are compared with two small eccentricity perturbation theories. Results show that load capacity and stiffness are generally less than theory predicts. Of the two theories, the pressure perturbation theory shows better agreement with the observed data. *Self-acting effects from journal* rotation are greatest at the higher eccentricity ratios and lower supply pressures. Results were obtained for speeds up to 25 000 rpm and radial loads were varied up to 20.2 psi (139 kN/m^2).

EXPERIMENTS ON ROTATING EXTERNALLY PRESSURIZED, AIR JOURNAL BEARINGS I - LOAD CAPACITY AND STIFFNESS

by Robert E. Cunningham, David P. Fleming, and William J. Anderson

Lewis Research Center

SUMMARY

A series of tests was conducted to determine the load and stiffness characteristics of a pair of orifice-compensated, externally pressurized journal bearings. The diameters were a nominal $2\frac{1}{2}$ inches (6.3 cm) and the length $3\frac{3}{4}$ inches (9.5 cm). Each bearing was equipped with 12, 0.022-inch (0.56-mm) diameter orifices. The orifices were arranged in two circumferential planes, six equally spaced in each plane.

Results were obtained at an average radial clearance of 0.00135 inch (0.034 mm) over a speed range of 0 to 25 000 rpm. Radial loads were varied up to 189 pounds (840 N) per bearing or 20.2 psi (139 kN/m^2) unit load and air supply pressure ratios from 1.7 to 6.

The results of these tests show that load capacity is generally less than that predicted by linearized PH theory or by pressure perturbation theory. Agreement is fair at eccentricity ratios up to 0.1 and at higher supply pressures. A comparison of test results with the two perturbation theories shows that the observed load capacity data agree better with the pressure perturbation theory. Overall load capacity is increased by shaft rotation (self-acting effects). The increase is greatest at the higher eccentricity ratios and lower supply pressures. Experimental data of stiffness as a function of compressibility number are in close agreement with theory at the higher supply pressures.

INTRODUCTION

Power requirements for future space programs, such as manned orbiting stations, lunar surface exploration, or unmanned interplanetary missions, could reach the 300-kilowatt level (ref. 1). Mechanical energy conversion systems employing advanced reactors will be larger than the 12- to 30-kilowatt systems currently being developed. Self-acting bearings (the partial-arc, tilting-pad design, currently used in Brayton cycle

turbomachinery) may become marginal with respect to load capacity. When this occurs it may become necessary to consider externally pressurized radial-gas bearings.

In an externally pressurized bearing, gas is fed through inlet restrictors, which are equally spaced circumferentially in one or more radial planes. Orifices are most commonly used as flow restrictors, although flow-control valves or capillaries may also be used (ref. 2). Pressure drops occur in the gas stream flowing through an orifice. They also occur in the gas flow through the curtain area (see fig. 4) around the orifice and into the bearing clearance annulus. The ratio of the orifice area to the curtain area is referred to as the inherent compensation factor and is given by the symbol δ. When δ becomes greater than one, the bearing is said to be inherently compensated. When δ approaches zero ($\delta \ll 1$), the bearing is said to be orifice compensated.

Much of the experimental research effort to date on externally pressurized bearings has been devoted to determining the zero-speed load capacity. Experimental results reported for rotating bearings have been limited to fairly low speeds (up to 7500 rpm). The results reported in reference 3 with a single, 2-inch (5.1-cm) diameter bearing did, however, point out the significant contribution to overall load capacity from shaft rotation.

Single and double plane orifice compensated, externally pressurized journal bearings have been treated analytically by J. Lund in references 4 and 5. The analyses assume a sufficient number of orifices in each feeding plane so that they can be approximated by a line pressure source. Both analyses use a perturbation technique. In reference 4 the perturbed variable is the product of film pressure and film thickness. This is generally referred to as the linearized PH theory. The perturbed variable in reference 5 is the pressure P. Furthermore, the analyses assume only small displacements of the rotor center from the bearing center. Because of the assumptions made in these analyses, the validity and range of applicability of the results must be determined from experimental work.

The results of this investigation are reported in two parts. The objectives of the first part of the investigation, reported herein, are (1) to determine experimentally the load capacity and film stiffness at varying supply pressures, (2) to examine more closely the effects of shaft rotation on load and stiffness at varying supply pressures, and (3) to compare the results obtained with available theories.

The second part of this experimental investigation (ref. 6) presents results for bearing attitude angles and measured air mass flows for the same range of conditions.

The results reported in this investigation were obtained with a pair of $2\frac{1}{2}$-inch (6.3-cm) diameter, $3\frac{3}{4}$-inch (9.5-cm) long orifice-compensated, externally pressurized air bearings. The rotor was operated in the two bearings at an average radial clearance of 0.00135 inch (0.034 mm). Rotor speeds were varied from 0 to 25 000 rpm (This corresponds to a range of compressibility numbers Λ from 0 to 2.8). Externally ap-

plied unidirectional loading varied up to 189 pounds (840 N) per bearing or 20.2 psi (139 kN/m^2) of projected area. Air supply pressures varied from approximately 24 to 88 psia (169 to 610 kN/m^2) which corresponds to supply pressure ratios P_s/P_a of 1.7 to 6.0.

APPARATUS

The test results reported in this investigation were obtained with the apparatus shown in figure 1. The two bronze test bearings were mounted in two stainless-steel plates. Three vertical arbors, with appropriate spacers, served to locate the bearing plates at a span of 8 inches (20.3 cm). The lower bearing plate was rigidly fixed on the arbors while the upper bearing plate could be moved laterally and angularly. This permitted alinement of the upper bearing with the lower bearing. Radial passageways in the plates supplied pressurized air to the bearing annuli which supplied the 12 orifice restrictors in each bearing (fig. 1(b)). The bottommost plate held an externally pressurized thrust bearing which supported the 24.5-pound (11.1-kg) rotor.

An externally pressurized air bearing, connected through a piv to the piston shaft of a pneumatic load cylinder, is used to apply a radial load midway between the two bearings (fig. 1(b)). The bearing surface has four rectangular recessed pokets, each with its own orifice restrictor (fig. 2).

The rotor is driven by pressurized air from two nozzles impinging on 30 buckets milled in the rotor surface at the upper end. An identical set of buckets at the lower end (cut in the opposite direction) acts as a brake when air is applied.

Test Bearings and Rotor

One of the externally pressurized bearings used in this investigation is shown with the test rotor in figure 3. It is $2\frac{1}{2}$ inch (6.3 cm) in diameter by $3\frac{3}{4}$ inches (9.5 cm) long giving a length to diameter ratio of $1\frac{1}{2}$. The bearings are made of SAE 68-B cast aluminum bronze and were precision machined before installation in the test apparatus. Geometry gage measurements of the bores showed roundness and concentricity to be within 40 microinches (1 μm). Each bearing has 12 orifice plugs arranged in two rows of six equally spaced around the circumference. The orifice planes are located one quarter of the way in from the bearing ends. Figure 4(a) shows the method by which the orifices are mounted. Figure 4(b) shows the relation of orifice length to diameter. The inherent compensation factor for this bearing is 0.46, making this bearing orifice compensated. The $2\frac{1}{2}$-inch (6.3-cm) diameter by 18-inch (46-cm) long rotor is made of

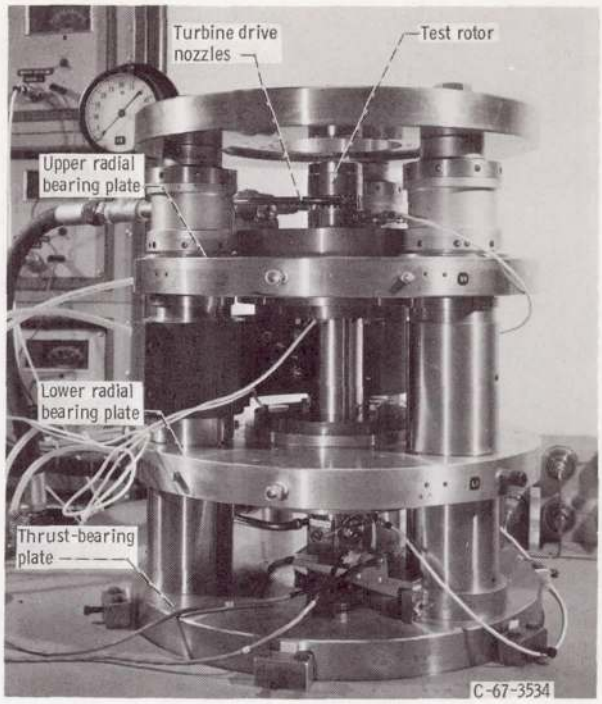

(a) Photograph.

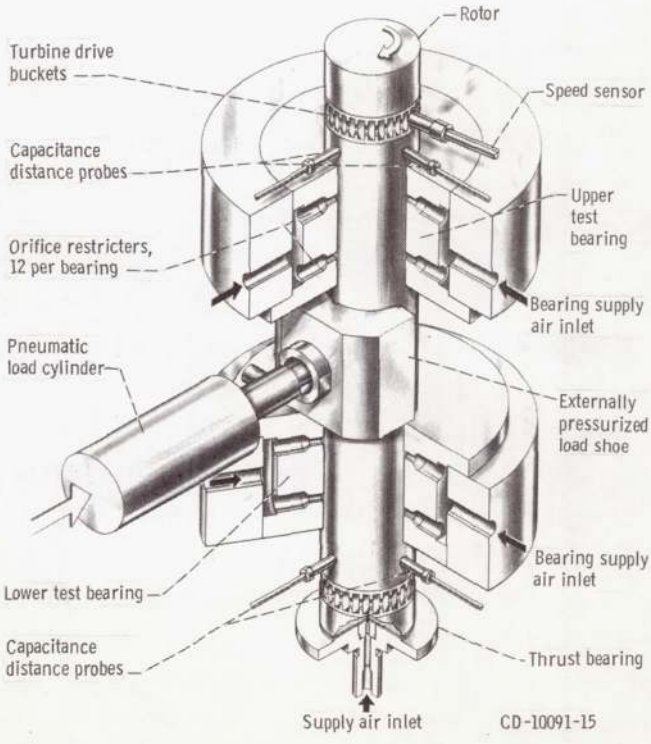

(b) Schematic

Figure 1. - Externally pressurized air bearing test apparatus.

Figure 2. - Partial-arc externally pressurized load shoe with four recessed pockets.

Figure 3. - Test bearing and rotor.

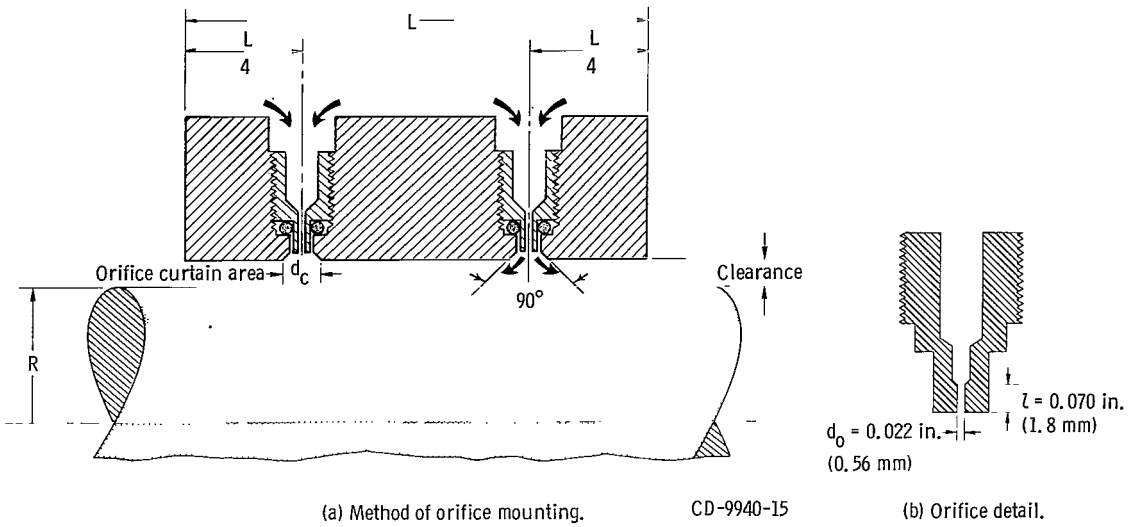

Figure 4. - Section view of test bearing.

consumable-electrode vacuum-melt SAE 52100 steel and weighed 24.5 pounds (11.1 kg). This material was chosen because of its good dimensional stability. To improve the surface characteristics and inhibit corrosion, the rotor was chromium plated. Measurements made of the rotor showed it to be round within 20 microinches (0.5 μm) and concentric within 50 microinches (1.3 μm) over the bearing lengths.

Instrumentation

Two orthogonally oriented capacitance distance probes were mounted outboard of each test bearing in the same radial plane (fig. 1(b)). These probes provided a noncontacting method of monitoring radial displacement of the rotor. Each of these probes, with its own capacitance distance meter, cables, and filters, was calibrated before installation in the test apparatus. Voltage output readings were read on a digital voltmeter. Values of 1 millivolt, corresponding to a distance of 5 microinches (0.1 μm) were readily discernible. An X-Y curve tracing oscilloscope was used to display the locus of the rotor center. Pressures were measured by strain gage transducers (accurate to 0.1 percent), and their output read on a digital voltmeter.

A solid-state electronic controller was used to regulate turbine air supply and maintain preset rotor speed to within 0.5 percent. Inductive type of sensors in close proximity to the turbine buckets monitored rotor speed.

PROCEDURE

Before each test, clearance measurements were made of each bearing using the capacitance distance probes. Dry, filtered air was then supplied to the bearings, and the pressures were adjusted to the same value in each bearing. Capacitance probe readings were recorded defining the zero load or concentric rotor position. Air to the turbine was supplied, and the rotor brought up to the desired speed. Radial loads were applied and displacements recorded. This procedure was repeated at different speeds until self-excited whirling of the rotor occurred at that value of supply pressure. At this point, the speed was reduced to 10 000 rpm, and a new value of supply pressure was adjusted; again, the procedure was repeated.

RESULTS AND DISCUSSION

Results are presented in figures 5 to 8. Dimensionless load capacity (or bearing efficiency) is plotted against eccentricity ratio for supply pressure ratios P_s/P_a of 2.3, 3.5, 4.8, and 6.0 for both the zero-speed and rotating cases in figure 5. Generally, it can be concluded that agreement between the experimental results and theory is poor at high eccentricity ratios or heavy loads. At the higher supply pressure ratios the pressure perturbation theory (ref. 4) could be used with fair accuracy for lightly loaded systems. The linearized PH theory (ref. 5) is not quite as good as the pressure perturbation theory as can be seen in figure 5(a) for $P_s/P_a = 2.29$. The slope of the experimental zero-speed load capacity curve decreases with increasing eccentricity ratio. This is characteristic of orifice compensated, externally pressurized bearings. The effect of shaft rotation on the load capacity of an externally pressurized bearing can be seen in figures 5(a) and (b). The increase in load capacity, particularly at the higher eccentricity ratios, is due to increased film pressures from self-acting effects. This suggests that a smaller clearance might enhance the self-acting contribution to load capacity. In fact, experimental results for an externally pressurized bearing with rotation (ref. 3) show that load capacity increases sharply at a clearance ratio C/R less than 0.6×10^{-3}. The radial clearance ratio for the bearing under investigation in this report is 1.04×10^{-3}. A comparison is made in figure 5(c) of experimental load capacities for the bearing of this investigation and the externally pressurized bearing of refer-

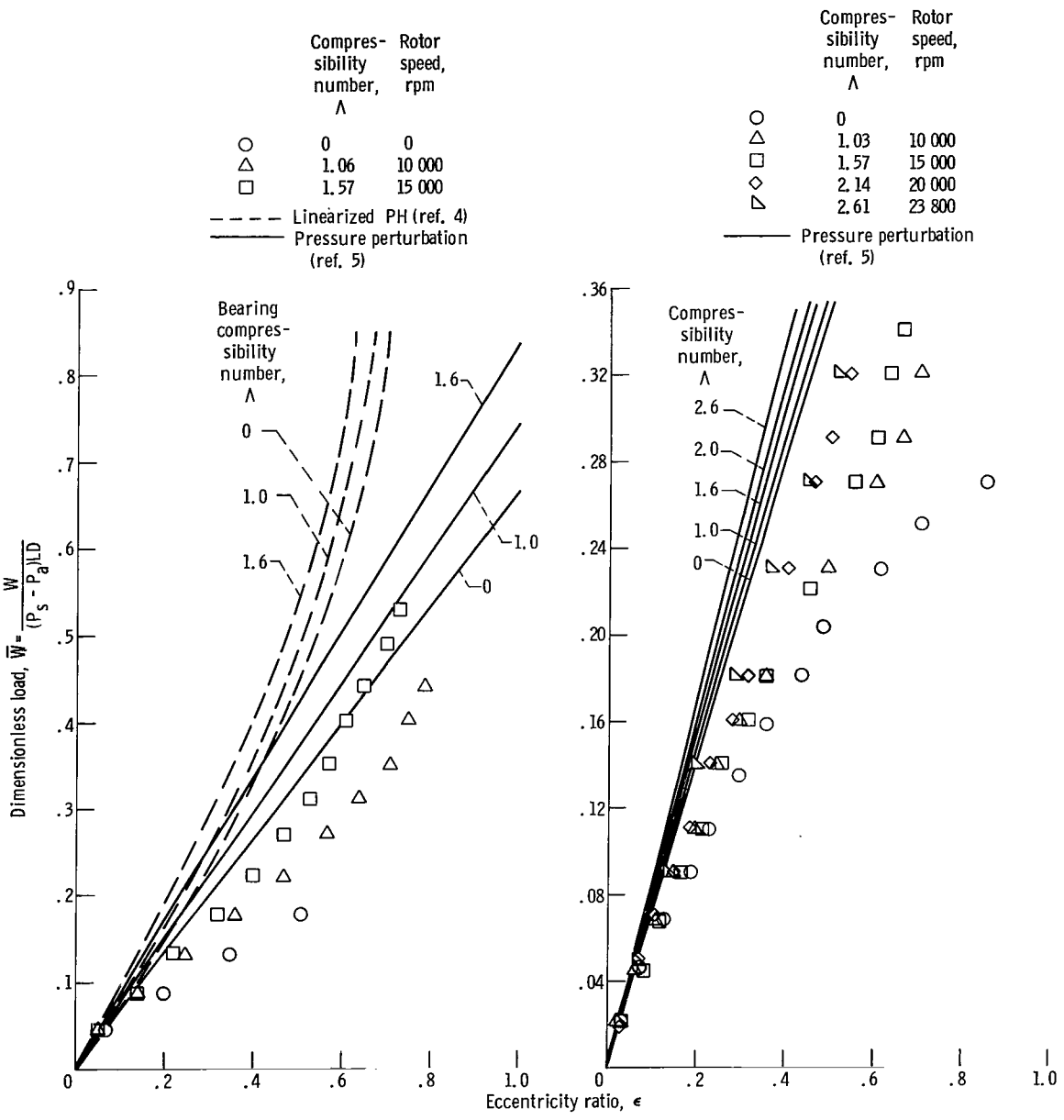

(a) Supply pressure ratio, 2.3.

(b) Supply pressure ratio, 3.6.

Figure 5. - Dimensionless load against eccentricity ratio. Rotor diameter, 2.5 inches (6.3 cm); atmospheric pressure, 14.4 psia (99 kN/m^2); bearing length, 3.75 inches (9.5 cm); number of orifices, 12; orifice diameter, 0.022 inch (0.56 cm); bearing radial clearance, 0.00132 inch (0.0335 mm).

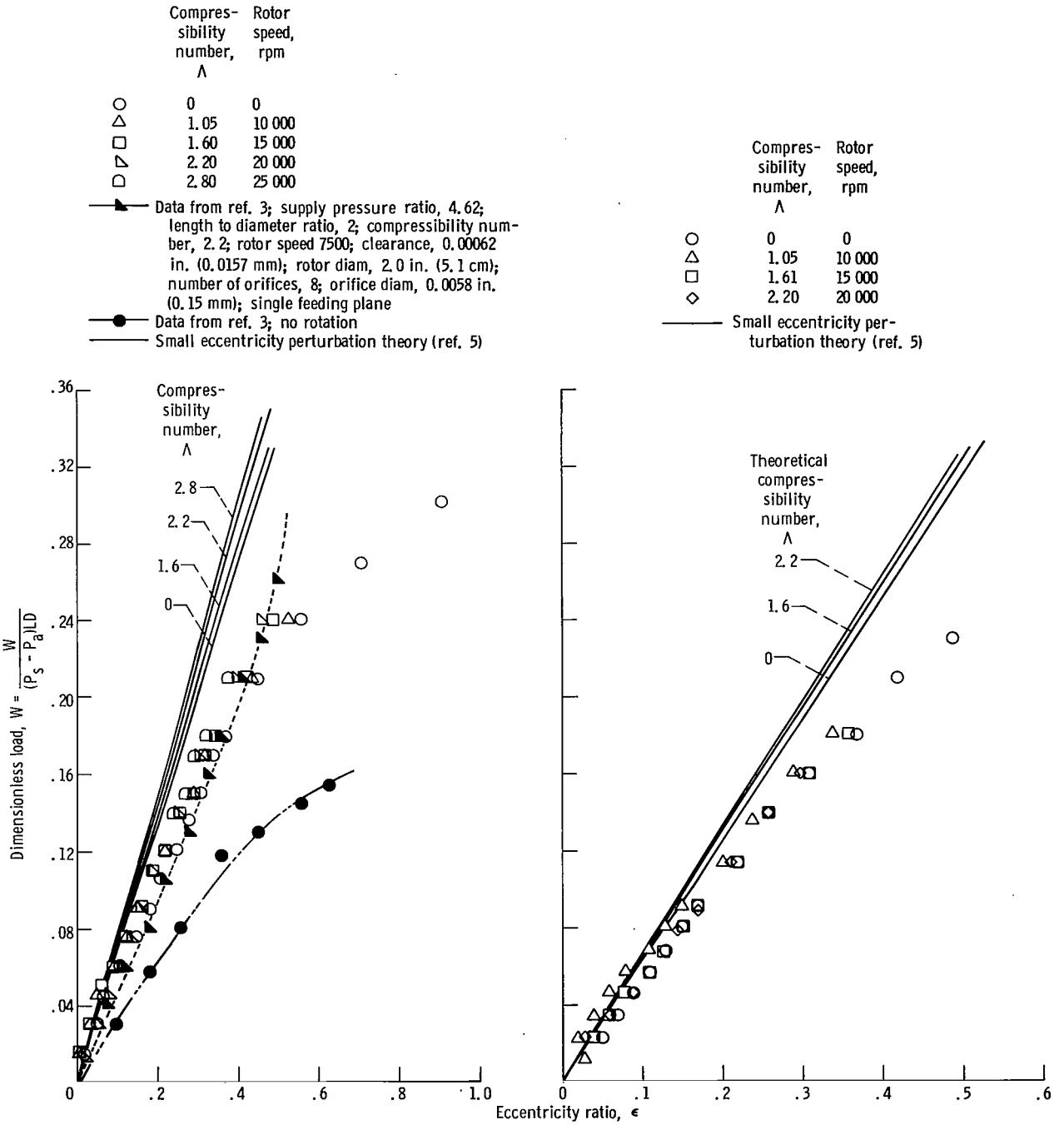

(c) Supply pressure ratio, 4.8.

(d) Supply pressure ratio, 6.0.

Figure 5. - Concluded.

ence 3. Supply pressure ratios are P_s/P_a = 4.9 and 4.6, respectively. The characteristic dimensions of the two bearings are listed in the following table:

Characteristic dimension	This investigation	Reference 3
Diameter, in.; cm	2.5; 6.3	2; 5.1
Length to diameter ratio, L/D	1.5	2
Clearance ratio, C/R	1.04×10^{-3}	0.62×10^{-3}
Number of feeding planes	2	1
Number of orifices per feeding plane	6	8
Diameter of orifices, in.; cm	0.022; 0.56	0.0058; 0.15

A comparison of the zero-speed load curves of figure 6(c) shows that the double feeding plane bearing has significantly greater load capacity than the single feeding plane bearing. However, at a compressibility number Λ of 2.2 the load capacities for the two bearings are almost identical. The obvious conclusion that can be drawn from this comparison is that the self-acting contribution is much greater at smaller clearances.

The results plotted in figure 5(d) for a supply pressure ratio of 6 show that agreement between experiment and theory is quite good up to an eccentricity ratio ϵ of 0.2. It is evident that there is no significant increase in load capacity due to shaft rotation at this high supply pressure ratio. Self-acting effects are completely masked by the higher film pressures from external pressurization.

Figure 6 shows how overall load capacity varies with bearing compressibility number at pressure ratios from 1.7 to 6 at an eccentricity ratio ϵ of 0.3. For all speed and pressure ranges investigated the experimental load capacity is always less than that predicted by the small eccentricity pressure perturbation theory. Agreement appears to be better at the higher supply pressures.

Figure 7 shows that the film stiffness at zero speed decreases with increasing eccentricity ratio. The stiffness at a given eccentricity is the slope of the load curve at that point. At zero shaft speed (Λ = 0) the load curve has a decreasing slope, which produces a decrease in the film stiffness. Film stiffness as a function of eccentricity ratio, as predicted by the pressure perturbation theory, would appear as a straight line parallel to the abscissa. The load curves for this theory are lines having constant slope. For the experimental load curves with rotation, the slope increases with eccentricity ratio at lower supply pressures and higher eccentricity ratios. This increasing slope is reflected in the stiffness curves of figures 7(a) to (c) and particularly at eccentricity ratios ϵ above 0.5.

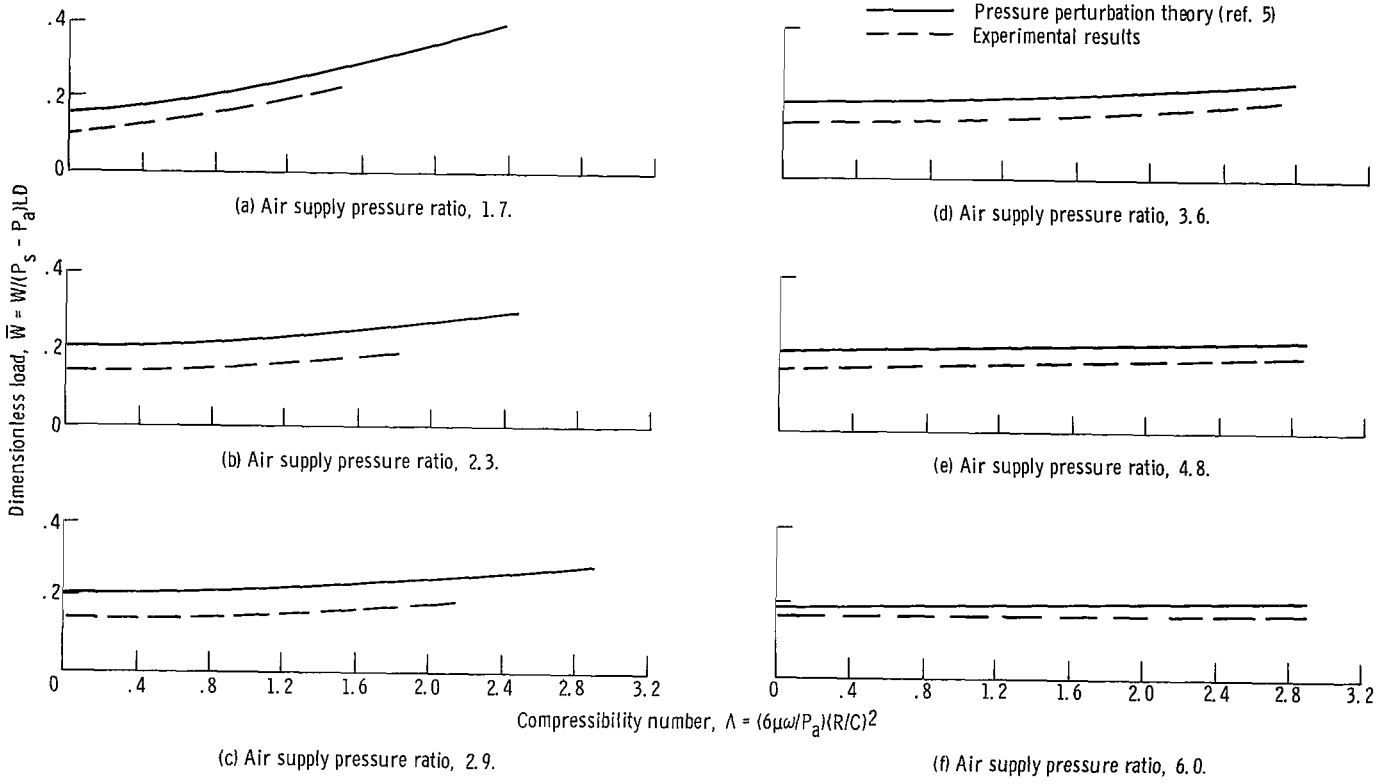

Figure 6. - Comparison between experimental and theoretical dimensionless load against compressibility number. Eccentricity ratio, 0.3; bearing length, 3.75 inches (9.5 cm); rotor diameter, 2.5 inches (6.3 cm); atmospheric pressure, 14.4 psia (99 kN/m^2); number of orifices, 12; orifice diameter, 0.022 inch (0.56 mm); average radial clearance, 0.00135 inch (0.0343 cm).

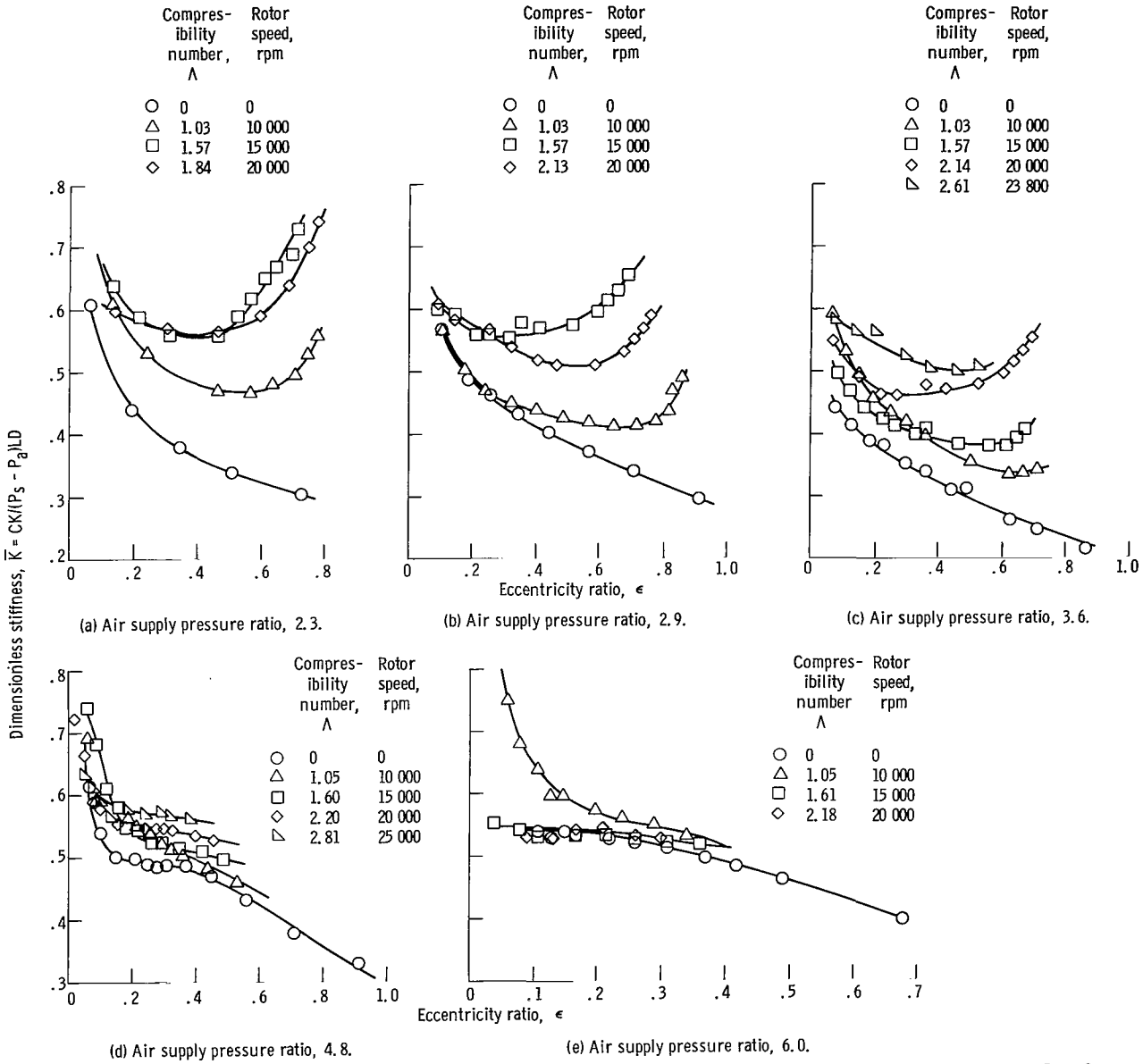

Figure 7. - Dimensionless stiffness against eccentricity ratio at various compressibility numbers. Atmospheric pressure, 14.59 psia (10^5 N/m^2); rotor diameter, 2.5 inch (6.3 cm); bearing length, 3.75 inch (9.5 cm); number of orifices, 12; orifice diameter, 0.022 inch (0.56 mm); clearance, 0.00132 inch (0.0335 mm).

Experimental film stiffness as a function of compressibility number is plotted in figure 8 for an eccentricity ratio ϵ of 0.1. The pressure perturbation theory shows a steady increase in stiffness with increasing compressibility number. This increase in stiffness due to shaft rotation decreases with increasing supply pressure, as did load capacity. This, however, is not true for the experimental values of stiffness. They appear to increase very slightly and then fall off. There is no definite trend of increasing stiffness for increasing compressibility number at small eccentricities as theory predicts.

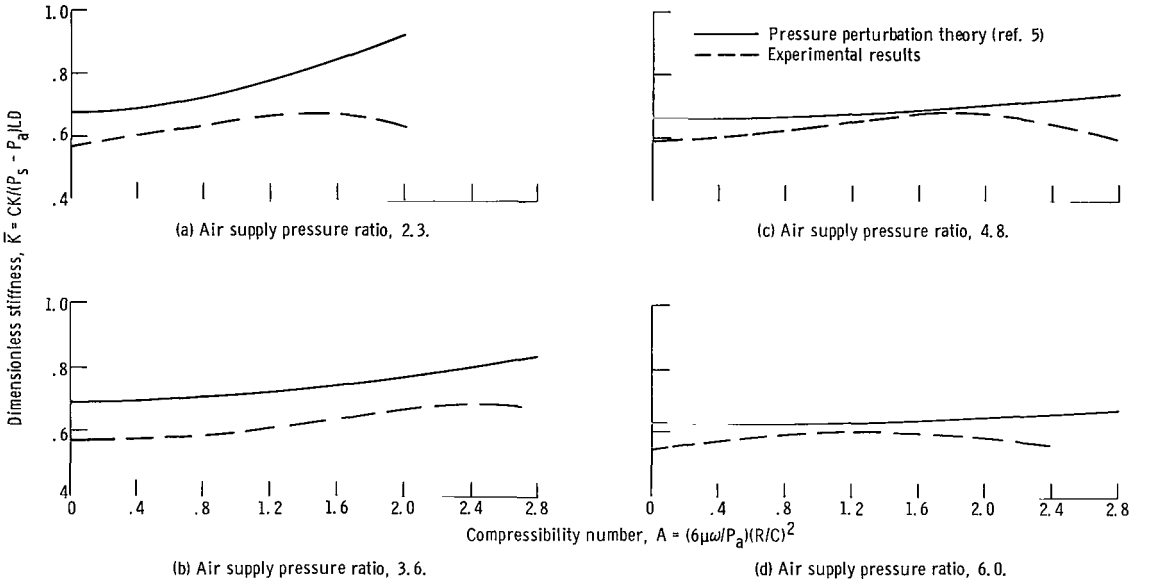

Figure 8. - Comparison between experimental and theoretical stiffnesses. Eccentricity ratio, 0.1; bearing length, 3.75 inches (9.5 cm); rotor diameter, 2.5 inches (6.3 cm); number of orifices, 12; orifice diameter, 0.022 inch (0.56 mm); average radial clearance, 0.00135 inch (0.0343 mm).

SUMMARY OF RESULTS

The following results were obtained from experiments conducted on a pair of $2\frac{1}{2}$-inch (6.3-cm) diameter by $3\frac{3}{4}$-inch (9.5-cm) long externally pressurized air lubricated bearings having an average 0.00135-inch (0.034-mm) radial clearance. The 18-inch (46-cm) long 24.5-pound (11.1-kg) rotor supported in the bearings was operated at speeds from 0 to 25 000 rpm corresponding to a range of compressibility numbers Λ from 0 to 2.8. Radial loads varied up to 189 pounds (840 N) per bearing or 20.2 psi (139 kN/m^2) of projected area. Air supply pressure ratios varied from 1.7 to 6. Eccentricity ratios varied from 0 to 0.9.

1. The load capacity or bearing efficiency is generally less than that predicted by two analyses, a pressure perturbation theory (ref. 5) and a linearized PH analysis

(ref. 4). Agreement is better at small eccentricity ratios and higher supply pressures

2. Of the two small eccentricity theories (pressure perturbation and linearized PH), the pressure perturbation theory shows better agreement with the observed data.

3. The percent of load capacity contributed by shaft rotation (self-acting effects) is greatest at the higher eccentricity ratios and lower supply pressures.

4. The stiffness of the bearing air film is increased due to shaft rotation. This increase in stiffness is significant at the lower supply pressures and particularly for eccentricity ratios above 0.5.

5. Theoretically predicted bearing film stiffness as a function of the bearing compressibility number is generally higher than the test results indicate. Agreement is better at the higher supply pressure ratios.

Lewis Research Center,
National Aeronautics and Space Administration,
Cleveland, Ohio, February 25, 1969,
129-03-13-05-22.

APPENDIX - SYMBOLS

C	bearing radial clearance, in.; mm
D	rotor diameter, in.; cm
d_c	curtain diameter, in.; mm
d_o	orrifice diameter, in.; mm
e	rotor eccentricity, in.; cm
K	bearing film stiffness, lb/in.; N/m
$\overline{K}$	dimensionless stiffness, $CK/(P_s - P_a)LD$
L	bearing length, in.; cm
l	orifice length, in.; mm
N	rotor speed, rpm
n	number of orifices
P_a	atmospheric pressure, psi N/m^2
P_s	bearing supply pressure, psi; N/m^2
R	rotor radius; in.; cm
W	applied radial load, lb; N
$\overline{W}$	dimensionless load, $W/(P_s - P_a)LD$
ϵ	rotor eccentricity ratio, e/C
δ	inherent compensation factor, $d_o^2/4d_cC$
Λ	bearing compressibility number, $(6\mu\omega/P_a)(R/C)^2$
μ	absolute viscosity, (lb)(sec)/in.^{2}; (N)(sec)/m^2
ω	rotor angular speed, rad/sec

REFERENCES

1. Lubarsky, Bernard; and Shure, Lloyd I.: Applications of Power Systems to Specific Missions. Space Power Systems Advanced Technology Conference. NASA SP-131, 1966, pp. 269-285.

2. Grinnell, S. K.; and Richardson, H. H.: Design Study of a Hydrostatic Gas Bearing with Inherent Orifice Compensation. Trans. ASME, vol. 79, no. 1, Jan. 1957, pp. 11-22.

3. Grassam, Norman S.; and Powell, J. W.: Gas Lubricated Bearings. Butterworth and Co., 1964, p. 171.

4. Lund, J. W.: The Hydrostatic Gas Journal Bearing With Journal Rotation and Vibration. J. Basic Eng., vol. 86, no. 2, June 1964, pp. 328-336.

5. Lund, J. W.: A Theoretical Analysis of Whirl Instability and Pneumatic Hammer for a Rigid Rotor in Pressurized Gas Journal Bearings. J. Lubr. Tech., vol. 89, no. 2, Apr. 1967, pp. 154-166.

6. Cunningham, R. E.; Fleming, D. P.; and Wm. J. Anderson: Experiments on Rotating Externally Pressurized Air Journal Bearings. II - Bearing Attitude Angle and Air Flow. NASA TN D-5192, 1969.

NASA-Langley, 1969 —— 15 E-4606

"The aeronautical and space activities of the United States shall be conducted so as to contribute . . . to the expansion of human knowledge of phenomena in the atmosphere and space. The Administration shall provide for the widest practicable and appropriate dissemination of information concerning its activities and the results thereof."

—NATIONAL AERONAUTICS AND SPACE ACT OF 1958

NASA SCIENTIFIC AND TECHNICAL PUBLICATIONS

TECHNICAL REPORTS: Scientific and technical information considered important, complete, and a lasting contribution to existing knowledge.

TECHNICAL NOTES: Information less broad in scope but nevertheless of importance as a contribution to existing knowledge.

TECHNICAL MEMORANDUMS: Information receiving limited distribution because of preliminary data, security classification, or other reasons.

CONTRACTOR REPORTS: Scientific and technical information generated under a NASA contract or grant and considered an important contribution to existing knowledge.

TECHNICAL TRANSLATIONS: Information published in a foreign language considered to merit NASA distribution in English.

SPECIAL PUBLICATIONS: Information derived from or of value to NASA activities. Publications include conference proceedings, monographs, data compilations, handbooks, sourcebooks, and special bibliographies.

TECHNOLOGY UTILIZATION PUBLICATIONS: Information on technology used by NASA that may be of particular interest in commercial and other non-aerospace applications. Publications include Tech Briefs, Technology Utilization Reports and Notes, and Technology Surveys.

Details on the availability of these publications may be obtained from:

SCIENTIFIC AND TECHNICAL INFORMATION DIVISION

NATIONAL AERONAUTICS AND SPACE ADMINISTRATION

Washington, D.C. 20546